THE EARTH RADIATION BELTS : NEW MODELS

Joseph Lemaire

Introduction

"The magnetosphere of the Earth extends about 10 Earth radii (RE) toward the Sun and over 1000 RE in the direction away from the Sun. Its outer boundaries and their deformation are attributed to the solar wind - the tenuous, ionized, magnetized gas (plasma) that flows outward from the solar corona through interplanetary space. The solar wind does not readily penetrate the geomagnetic field but compresses and confines the field around the Earth" (Van Allen, 1991). The sunward boundary of the magnetosphere is located where the kinetic energy associated to the incident bulk velocity of the solar wind is completely converted into thermal motion (i.e. gyromotion of the ions and electrons) in the geomagnetic field. At this surface called the magnetopause the external pressure of the flowing solar wind equals the internal pressure of the geomagnetic field. The electromagnetic interaction of the solar wind's magnetic field and the geomagnetic field stretches out the magnetic field in the direction away from the Sun, creating a long magnetotail.

Radiation Belts are formed in the interior of the magnetosphere. They comprise a population of energetic, electrically charged particles (electrons, protons and heavier atomic ions) stably trapped in the magnetic field of the Earth. In this context the term energetic means kinetic energies $E \geq 30$ keV. Although, these energetic particles donot contribute significantly to the magnetospheric plasma density which is mainly due to particles of 10 eV up to 30 keV, they constitute an important population of particles indeed they damage space systems.

General description of radiation belts

"A radiation belt is toroidally shaped, encircles the Earth, and its axis of rotational symmetry is coincident with the magnetic dipolar axis of the Earth. To a first approximation, each particle therein moves with constant energy and independently of all other particles along a helical path encircling a magnetic field line. This motion is determined by the Lorentz force of a static magnetic field on a moving electrically charged particle, namely $q(v \times \mathbf{B})$, where q is the particle's electrical charge, v its velocity, and **B** the local magnetic field intensity. The angle between v and **B** is called the pitch angle. It tends toward either 0° or 180° at the magnetic equator during each latitudinal excursion and becomes 90° at mirror or reflection points in the northern and southern hemispheres as the particle penetrates into the stronger magnetic field near the Earth. The helix drifts slowly in longitude, westward for $q < 0$ (protons and other ions) and eastward for $q > 0$ (electrons), so as to generate the overall toroidal shape of the trapping region" (Van Allen, 1991).

The azimuthal motion of ions and electrons in opposite directions produces a huge Ring Current which is responsible for the decrease of the horizontal component of the equatorial magnetic field intensity, during geomagnetic storm events.

The trajectory of ions of very high energies in a dipole magnetic field can be very complex. It was studied for the first time by K. Störmer at the beginning of this century. He solved numerically the mechanical equation of motion of charged particles in a dipole magnetic field distribution, for a wide range of initial conditions.

Departures from the trajectories calculated by the theory of Störmer are caused by the presence of thermal and nonthermal ionized gas (plasma) that causes a large variety of cooperative physical phenomena, essential to understanding magnetospheric dynamics. In analyzing such processes the Störmerian approach is usually supplanted by characterizing a particle's motion with three adiabatic invariants, corresponding to the three cyclic components of motion having widely different periods, namely, gyration around B (~milliseconds), latitudinal oscillation (~seconds), and longitudinal drift (~hours).

The magnetospheric properties define the external environment. The energetic particle population may place important constraints on the practicality of in situ measurements and on the survival of electronic and optical equipment, human flight crews, animals, and other life forms flown in it. The particle population of the Earth's radiation belts makes it dangerous for humans without massive shielding. This is why it is so important from a technological point of view, to build empirical and physical

models of this energetic particle environment of the Earth.

The diverse particle phenomena in the Earth's magnetic field have been studied intensively, both observationally and theoretically, since Van Allen's discovery of their existence in 1958. The minimum condition for the existence of a planetary radiation belt is that the planet's dipole magnetic moment be sufficiently great that the flow of the solar wind is arrested before it reaches the top of the appreciable atmosphere or surface of the planet. Durable trapping of charged particles is possible only if this condition is met. Otherwise, particles are lost quickly by collisions with atmospheric gas or have open Störmerian trajectories.

Sources of radiation belt particles

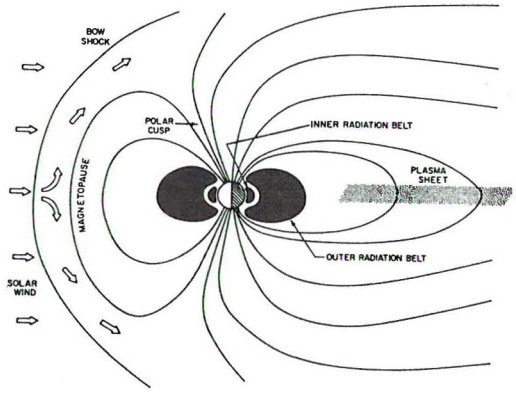

Figure 1 : Illustration of the magnetosphere of the Earth. The Van Allen radiation belts containing very energetic electrons and ions are shown in the inner magnetosphere as black areas (after Van Allen, 1991)

The radiation belts and other features of the Earth's magnetosphere are shown to approximate scale in the noon-midnight meridian plane cross section of figure 1. The inner and outer radiation belts are two distinct features, defined by the intensity of particles capable of penetrating a specific shield (~ 1 g cm^{-2} of aluminium). In a generalized sense, there are as many different radiation belts as there are different species of particles and energy ranges that one wishes to distinguish. The principal sources of particles for the outer belt are the solar wind and the ionosphere; for the inner belt, sources are electrons and protons from the in-flight radioactive decay of neutrons from nuclear reactions produced by galactic cosmic rays and solar energetic particles in the tenuous gas of the upper atmosphere. The eventual fate of magnetospheric particles is to become part of the atmosphere, to collide with satellites or particulate matter in planetary rings, or to escape into space. The first two sources of particles are responsible for most of the gross geophysical manifestations of the magnetosphere (aurorae, geomagnetic storms, and heating of the upper atmosphere). The third is responsible for the relatively stable population of very energetic protons and some of the energetic electrons in the inner radiation belt. It should be pointed out that this third source would produce a radiation belt around a magnetized planet even if the solar wind did not exist.

The residence times of individual particles in the radiation belts of Earth, controlled by ionization losses in the atmosphere near the Earth (at altitudes less than 400 km), increase rapidly to the order of years at a radial distance of about 8,000 km (1.25 Earth radii), then decline in a complex and time-variable way to values of the order of weeks, days, and minutes in the outer fringes. There are quite low intensities of radiation belt particles within a spherical shell of about 400 km thickness around Earth. This is the region of space flight that is relatively safe from the radiation point of view. The inner radiation belts extends from this lower boundary to an equatorial radial distance of about 12,000 km and the outer radiation belt from this point outward to about 60,000 km. There is considerable overlap of the two principal belts and a complex and time-variable structure in the outer one. Some sample omnidirectional intensities are
$J = 2 \times 10^4$ cm^{-2} s^{-1} of protons $E_p > 30$ MeV in the most intense region of the inner belt; and
$J = 3 \times 10^8$ cm^{-2} s^{-1} of protons $E_p > 0.1$ MeV,
$J = 2 \times 10^8$ cm^{-2} s^{-1} of electrons $E_e > 0.04$ MeV, and
$J = 1 \times 10^4$ cm^{-2} s^{-1} of electrons $E_e > 1.6$ MeV in the most intense region of the outer belt.

Coordinate systems to map radiation belt fluxes

Radiation belt fluxes usually are mapped in a geomagnetic coordinate system (B, L) introduced by McIlwain (1961). B is the magnetic field intensity at the point of measurement and L is a parameter determining the drift shell (B, L) of a trapped particle with pitch angle equal to 90° at the point of observation. For particles mirroring at this point B and L are invariants of motion, uniquely determined in terms of the first and second adiabatic invariants of motion μ and I (McIlwain, 1961). The adiabatic invariants associated with the motion of a particle not mirroring at the point of observation are the mirror point magnetic field intensity $B_m \equiv B/\sin^2\alpha$ and L_m, the L parameter obtained by tracing the field line passing through the point of observation down to the mirror point.

The position and shape of a drift shell of trapped particles is determined by the geomagnetic field distribution and the pitch angle α at the point of observation; it is completely described by the coordinate pair (B_m, L_m).

At the Institute for Space Aeronomy the TREND-2 research team has developed, under ESA-ESTEC contract, a new computer program called BLXTRA, which enables one to determine the pair of coordinates (B_m, L_m) of a magnetic drift shell for any value of the pitch angle (α); i.e. for any orientation of the view angle of a charge particle telescope. This improvement has been implemented in the UNIRAD software used by ESA and in the European Aerospace Industry for the calculation of expected radiation doses for a planned space mission. It enables us to map directly directional flux measurements in (B_m,L_m) space, and then to build more sophisticated and reliable radiation belt models.

D. Heynderickx, working for the TREND-2 project, has used this new software package to analyse and to map directional fluxes of protons of 1 MeV to 100 MeV, which have been measured with the satellites AZUR and CRRES. Figure 2 illustrates the distribution of proton fluxes of 1 MeV in (B_m,L_m) space (Lemaire et al., 1995).

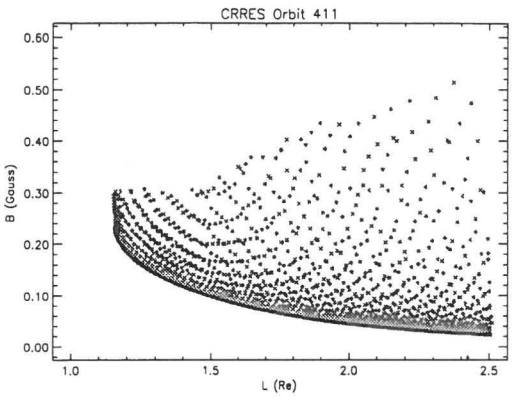

Figure 2 : The outbound trajectory of the CRRES spacecraft is shown by the solid line in (B,L) space. The dots correspond to the values of (Bm, Lm) corresponding to the mirror points of particles with different pitch angles sampled by the PROTEL proton detector during successive spin periods (after Lemaire et al., 1994)

The new BLXTRA code has already been used at Mullard Space Science Laboratory (MSSL) in England, as well as at Max Planck Institute for Aëronomie (MPI-Ae) in Germany to analyse and to map the fluxes of trapped electrons observed in the outer radiation belt with METEOSAT, CRRES and ISEE-2.

Secular variation of the geomagnetic field

The geomagnetic field distribution undergoes changes on different time scales including a slow secular variation. This slow secular variation of the geomagnetic field, consists of a decrease in the geomagnetic dipole moment (0.5% per century), a change in tilt angle of the geomagnetic axis (6.5 arcmin per decade), an increase of the eccentric distance of the centre of the Earth's dipole (2.8 km per year), and secular variations of all higher order moments. Hence, the (B_m, L_m) values for a fixed point in space and a given pitch angle will change with time. The ensuing secular variation of the (B, L) coordinates has important consequences for the mapping of trapped particle fluxes at low altitudes, i.e. below about 2000 km.

Until recently, scientists and aerospace engineers would use a geomagnetic field model extrapolated to an epoch which did not correspond to the epoch of 1960-1970 when the standard NASA empirical models were built based on measurements made in the 60's. The first TREND study recommended calculating (B, L) with the same geomagnetic field models was used to build the trapped particle models originally (Lemaire et al., 1991).

However, because of the secular variation of the geomagnetic field distribution some care should be taken when applying the NASA models AE8 and AP8 for contemporary flux calculations, especially for low altitude missions. In the present TREND-2 study, we found and recommended that the Jensen & Cain (1962) model should be used with AP-8 MIN, AE-8 MIN and AE8 MAX, and the GSFC 12/66 magnetic field model (Cain et al., 1967) with AP-8 MAX. The UNIRAD software has been adapted to automatically accomodate this recommendation. Since these NASA models were built more than twenty years ago, the location of the SAA has shifted considerably to the West due to the secular variation of the geomagnetic field distribution. The effect of this westward shift of the SAA can be compensated by applying an eastward rotation to the geographic coordinates of the points where the flux is to be estimated (Lemaire et al. 1995). This feature has been implemented in UNIRAD as well.

Comparison of the NASA and the Russian INP radiation belt models

Since the discovery of the radiation belts by Van Allen in 1958, the omnidirectional flux of protons and electrons has been measured at all relevant energies (E) by different types of particle detectors flown in all regions of the magnetosphere.

The first empirical models of the radiation environment were designed in the early 60's at Aerospace Corporation and later on at NSSDC by J.I. Vette and his colleagues

(Vette 1991b). The latest versions of the NASA electron models are called AE-8 MIN and AE-8 MAX (Vette 1991a). They are valid for conditions of minimum and maximum solar activity, respectively. The corresponding proton models are AP-8 MIN and AP-8 MAX (Sawyer & Vette 1976). The E, L, B dependence of the omnidirectional proton and electron fluxes is stored as a three dimensional array (Vette 1991a).

Trapped radiation belt models similar to the NASA models AP-8 and AE-8 have been produced in the Soviet Union to evaluate the radiation dose on future missions. As part of the TREND-2 study, we have evaluated the models developed at the Institute of Nuclear Physics of the Moscow State University (INP/MSU). The INP models have been compared to the NASA models in a Technical Note by Beliaev and Lemaire (1994).

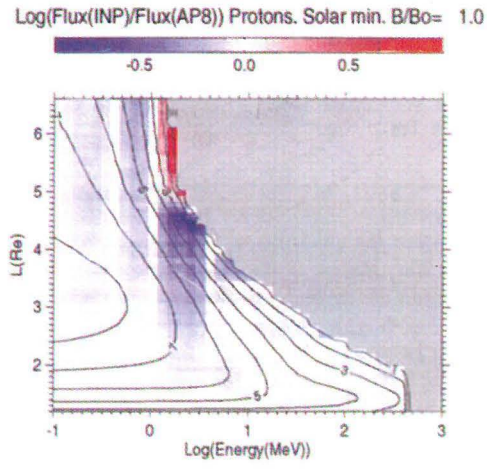

Figure 3 : Comparison between the Russian INP and the NASA AP8-MIN radiation belt models for solar minimum. The solid lines are iso-contours of omnidirectional fluxes versus energy (horizontal axis) and versus L (vertical axis) for the AP8-MIN model. The Russian model gives larger fluxes where the pixels are coloured in red. The NASA model gives larger fluxes where the pixels are coloured in blue according to the intensity scale shown on top of the figure (after Beliaev and Lemaire, 1994).

Figure 3 shows the omnidirectional flux distribution of trapped protons versus L (in Earth's radii) and as a function of the energy E (in MeV). The isoflux contours shown by solid lines correspond to the AP8-MIN model developed in the 60's by NASA for minimum solar activity conditions. The difference of the Logarithm of these fluxes with the corresponding quantities given by the Russian INP-PRMIN model is illustrated by the red and blue colour intensity scaled in the top panel in a scale proportional to the logarithm of the flux ratio. Red is where the Russian model gives a higher flux than the American model. Blue is where the AP8-MIN flux is larger than the INP-PROTMIN flux. White is where both results give the same values.

It can be seen that both models agree satisfactorily in most region of the (L,E) space, except near the grey shaded areas where the fluxes are below the detection thresholds. In this region the flux is relatively small and has steep spatial gradients in L and B. Other differences between both models are due to the different distributions of grid points in both models. Additional satellite observations have also been employed to update the INP models.

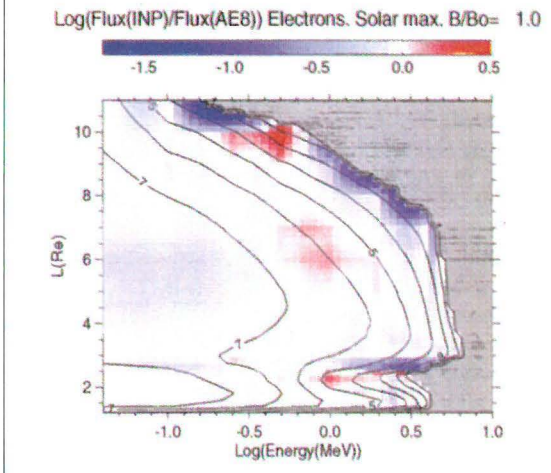

Figure 4 : Comparison between the Russian INP and the NASA radiation belt models for solar maximum. The solid lines are iso-contours of omnidirectional fluxes versus energy (horizontal axis) and versus L (vertical axis) for the AE8-MAX model. The Russian model gives larger fluxes where the pixels are coloured in red. The NASA model gives larger fluxes where the pixels are coloured in blue according to the colour scale shown on top of the figure (after Beliaev and Lemaire, 1994)

The same format is used in figure 4 to illustrate the differences between the omnidirectional fluxes of electrons predicted by the AE8-MAX model and the INP-EL-MAX model of the Russian Institute for Nuclear Physics. The solid lines correspond again to isoflux contours of the American model.

Although there are a few regions in (L,E) space where the electron fluxes of both models differ by more than a factor of two, however, in the heart of the radiation belts where the flux is highest, the American and Russian models give quite comparable results within a factor of two.

Atmospheric cut-off

From figures 3 and 4 it can be seen that large flux gradients are present at the inner edges of the radiation belt i.e. at smallest L-values where the trapped particles are most efficiently scattered in the loss cone by collisions with atmospheric atoms. The distribution of trapped protons at the inner edge of the radiation belt is most sensitive to the distribution of atmospheric constituents versus altitude. Since the atmospheric density depends on its heating rate by solar UV radiation, it is not surprising that the altitude distribution of the trapped proton flux is a function of the level of solar activity, at least in the altitude range between 300 km and 2000 km.

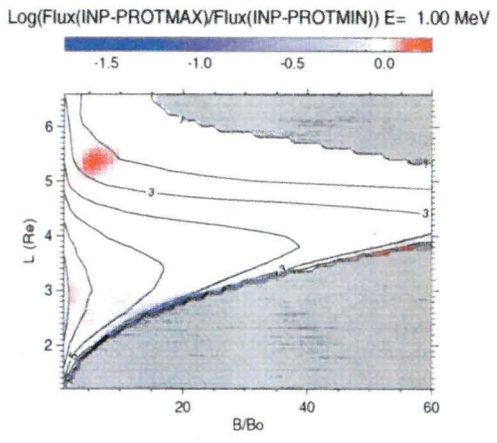

Figure 5 : Comparison between the AP8-MIN and AP8-MAX radiation belt models for solar minimum and solar maximum conditions. The solid lines are iso-contours of omnidirectional fluxes versus energy (horizontal axis) and versus L (vertical axis) for the AE8-MAX model. The AP8-MIN model gives larger fluxes in the region where the pixels are coloured in red. The AP8-MAX model gives larger fluxes where the pixels are coloured in blue according to the intensity scale shown on top of the figure (after Beliaev and Lemaire, 1994)

Figure 5 illustrates in the same format as used for figure 3, the differences between the proton fluxes in the Russian INP model for maximum and minimum solar activity conditions. It can be seen that near the surface of the Earth (i.e. for L<1.5) the proton flux at all energies is significantly larger during solar minimum than during solar maximum condition. This is a consequence of the larger flux of UV reaching the atmosphere, heating it and increasing its density at a given altitude.

Furthermore, during the TREND-2 study, we have shown that for L<1.5 both the fluxes given by the AP8-MIN and AP8-MAX models fit each other, providing, one uses another coordinate instead of B, to map their distribution versus altitude along a fixed magnetic field line. This new coordinate originally suggested by Hassitt (1965) is n_{av}, the drift shell averaged atmospheric density. This result indicates that the drift shell averaged atmospheric density may constitute a convenient new coordinate to map the distribution of energetic protons in the range of altitudes of the Space Shuttle, the MIR station and the future Space Station.

To confirm this far reaching conclusion we plan to use in the TREND-3 project this new coordinate for future development of a new type of radiation belt models based on AZUR and DMSP satellite data.

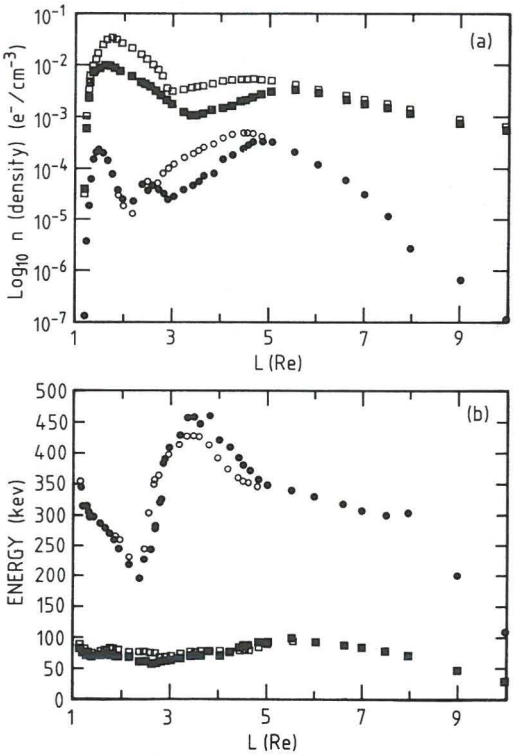

Figure 6 : Number density (top panel) and characteristic energy (bottom panel) of soft electrons (square symbols) hard electrons (circles) trapped in the inner and outer radiation belts according to the AE8-MIN (solid symbols) and AE8-MAX (open symbols) (after Pierrard and Lemaire, 1994)

Energy spectra of energetic electrons trapped in the magnetosphere

Pierrard and Lemaire (1994) have studied the energy spectrum of Van Allen electrons in the range between 100 keV and 4 MeV. They showed that the velocity distribution of these relativistic electrons can be represented by the superposition of two maxwellian functions. The temperatures and densities of these two electron populations vary with the radial distance. The soft electrons with the lowest temperature (70-90 keV) dominate the

inner electron zone, while the harder electron spectra corresponding to higher temperatures (250-450 keV) dominate in the outer electron zone. This is illustrated in figure 6 which shows the number densities (top panel) and characteristic energy (bottom panel) for both electron populations as a function of L. The squares correspond to the lower energy electrons (soft electrons) and the circles correspond to the high energy electrons (hard relativistic electrons). The solid and open symbols correspond respectively to the AE8-MIN and AE8-MAX models.

Conclusions

We have described above a few of the results obtained at the Institute for Space Aeronomy, Brussels, by the TREND and TREND-2 research teams. The software which has been developed as part of ESA contracts, to calculate the pitch angle dependent (Bm, Lm) drift shell coordinates as well as the n_{av} drift shell averaged atmospheric density, will be most useful in future radiation belt modelling efforts. Updated and new types of radiation belt models are needed to replace the over twenty years old NASA models. Such new models of the ionising radiation environment needed to improve the prediction of the energy spectra and dose of radiation accumulated behind the shield of any space vehicle orbiting in the magnetosphere are now available. These new models are useful to calculate the expected lifetime and deterioration of photovoltaic solar panels, and other sensitive electronic equipment; accurate and reliable radiation belt models are also required to plan mission operation for manned space vehicles as well as for astronomical observatories on GTO orbits traversing the harsh radiation zones.

Besides these software and empirical model improvement, what is now most needed is additional data sets collected over long periods of observation from different platforms orbiting simultaneously in different regions of the magnetosphere. Such comprehensive multi-point observations will be able to test and improve existing empirical models. They are useful to elaborate realistic physical models of the Earth's radiation environment. To achieve these goals extensive observation campaigns and surveys should be undertaken using minimally intrusive particle detectors on future spacecraft, as well as on mini-satellites dedicated and specially equiped to monitor the Earth's radiation environment.

Acknowledgements

I wish to thank ESA, and especially Dr. E.J. Daly , ESTEC technical manager for the TREND and TREND-2 projects 9828/92/ML/FM and 9011/88/ML/MAC, which enable the Belgian Institute of Space Aeronomy (BISA) to undertake this work.

References

BELIAEV A., J. LEMAIRE (1994), Evaluation of IMP Radiation Belts models, TREND-2, Technical Notes A, IASB, 3 Ave Circulaire, B-1180 Brussels, Belgium.

CAIN J.C., S.J. HENDRICKX, R.A. LANGEL, W.V. HUDSON (1967), A proposed model for the International Geomagnetic Reference Field-1965, *J. Geomagn. and Geoelectricity*, 19, 335.

HASSITT A. (1965), Average effect of the atmosphere on trapped protons, *J. Geophys. Res.*, 70, 5385-5394.

HEYNDERICKX D., J. LEMAIRE, Description of the combined release and radiation effects. Satellite experiments and data sets, Technical Note 4 of the TREND-2 study, ESTEC Contract 9828/92/ML/FM.

JENSEN D.C., J.C. CAIN (1962), An interim geomagnetic field, *J. Geophys. Res.*, 67, 3568.

LEMAIRE J., M. ROTH, J. WISEMBERG, P. DOMANGE, D. FONTEYN, J.M. LESCEUX, G. LOH, G. FERRANTE, C. GARRES, J. BORDES, S. MCKENNA-LAWLOR, J.I. VETTE, Development study of improved models of the Earth's radiation environment, Final Report of TREND, ESTEC contract 9011/88/ML/MAC.

LEMAIRE J., A.D. JOHNSTONE, D. HEYNDERICKX, D.J. RODGERS, S. SZITA, V. PIERRARD (1995), *Trapped radiation environment model development, TREND-2*, Final Report, ESTEC contract N° 9828/92/NL/FM; also *Aeronomica Acta A* - 386.

MCILWAIN C.E. (1961), Coodinates for mapping the distribution of magnetically trapped particles, *J. Geophys. Res.*, 66, 3681.

PIERRARD V., J. LEMAIRE, Fitting the AE-8 energy spectra with two maxwellian functions, Aeronomica Acta A383, 1994, to be published in Nuclear Tracks radiat. meas.

SAWYER D.M., J.I. VETTE (1975), The use of the inner zone electron model AE-5 and associated computer programs, NSSDC/WDC-A-R&S 72-11.

VAN ALLEN J.A. (1991), Why radiation belts exist, EOS, 72, 361-362.

VETTE J.I. (1991a), The AE-8 trapped electron model environment, NSSDC/WDC-A-R&S 91-24.

VETTE, J.I. (1991b), The NASA/National Space Science data center. Trapped radiation environment model program (1964-1991), NSSD/WDC-A-R&S 91-29.